Pergamon

Cement and Concrete Research 32 (2002) 363–371

CEMENT AND CONCRETE RESEARCH

Relationship between brittleness and moisture loss of concrete exposed to high temperatures

Binsheng Zhang*, Nenad Bicanic, Christopher J. Pearce, David V. Phillips

Department of Civil Engineering, University of Glasgow, Rankine Building, Glasgow G12 8LT, Scotland, UK

Received 7 July 2000; accepted 12 September 2001

Abstract

The effect of moisture loss at high temperatures on the brittleness of concrete was investigated by conducting three-point bending tests on preheated notched beams. The relationships of moisture loss represented by mass loss with heating temperature and exposure time could be established. Higher heating temperature always led to higher mass loss and lower brittleness. Longer exposure time led to higher mass loss and lower brittleness, but this effect was more significant at the early exposure stage and became insignificant thereafter. When concrete is exposed to high temperatures, the brittleness is reduced. The evaporation of gel water was more closely related to the brittleness.

Keywords: Concrete; High temperature; Exposure time; Brittleness; Mass loss

1. Introduction

Strength, stiffness, toughness, and brittleness are fundamental fracture properties of concrete. Strength and stiffness are directly used for the design and analysis of concrete structures under varied loading and environmental conditions. Toughness and brittleness are mainly used for the development of high-strength, high-performance concrete. Attempts have been made on using these two properties for the design and analysis of concrete structures. *Toughness* commonly characterizes the capacity of a material to resist deformation and fracture. So far, fracture toughness has been used to predict the fatigue life of cement concrete pavements [1] and to analyse cracking and stability of mass concrete dams [2]. *Brittleness* is commonly understood to be the tendency for a material or structure to fracture abruptly before significant irreversible deformation occurs. *Ductility* is the reverse of brittleness. Structures made of plain concrete are usually designed in accordance with the theory of elasticity or linear elastic fracture mechanics because the concrete is brittle, while structures made of steel and reinforced concrete, which are regarded as ductile, are normally designed in accordance with the theory of plasticity. Brittleness or ductility depends not only on the materials but also on the size of components. This means that design against brittleness is not only a pure material design but also an integrated material and structure design. The advent of high-strength concrete has led to new, cheap, high-performance structures, but in many cases led to big disappointments because the concrete has proved to be extremely brittle and unusable for loading–carrying structure. Design of such structures has also gone beyond the limits of the existing concrete code even though the concept of brittleness has also been used to design the new, ultra-strong, cement-based materials and assess failure mode of the components made of these materials [3]. The research on the concrete brittleness indeed helps further understand cracking and failure of conventional concrete materials and structures, helps develop new extremely strong and ductile materials and achieve better and more logical and holistic design. So far, the information about the concrete brittleness is very limited and few parameters are used to assess this property.

Much attention has been paid to these fundamental properties of concrete at room temperature. Research on these properties under elevated temperatures only started

* Corresponding author. Tel: +44-141-330-5919; fax: +44-141-330-4557.

E-mail address: zhang@civil.gla.ac.uk (B. Zhang).

0008-8846/02/$ – see front matter
PII: S0008-8846(01)00684-6

two decades ago and much progress has been made [4–12]. In general, the strength and stiffness of concrete decrease but the toughness increases with increasing heating temperature, exposure time, and thermal cycles. Accordingly, the concrete becomes less brittle. Information about these properties is extremely useful for the design of special concrete structures sustaining various high-temperature environments such as those for nuclear reactors, in the chemical industry, and for fire protection.

Previous research [4–6,8–11] acknowledges that the changes in fracture properties at high temperatures are related to the evaporation of moisture in concrete, physically or chemically. However, the effect of moisture in concrete on these fracture properties at high temperatures has not been systematically studied. The presence of water allows these properties to develop with time through the w/c and the degree of hydration. According to the sizes of pores it fills, the water in concrete can be classified as capillary water, gel water, and chemically combined water. Capillary water is readily evaporable water and exists not only in capillary pores (100–2000 Å) of cement paste but also in aggregate pores and at interfaces. It can easily evaporate when the relative humidity is low or the ambient temperature is high. Gel water exists in the gel pores (15–20 Å) of cement paste. It is generally described as adsorbed water or physically bound water and does not evaporate easily. However, it can be driven out when the ambient temperature is high so it is regarded as conditionally evaporable water. Chemically combined water, also called nonevaporable water, is part of the cement hydrate compounds and can only be released from concrete when the chemical decomposition of the cement paste and aggregates occurs at very high temperatures (over 500 °C). These three types of water are often called macro, meso, and micro water. The evaporation of capillary and gel water in concrete at high temperatures is a moisture loss process, but the decomposition of the cement paste and aggregates occurring at very high temperatures can also be regarded as a moisture loss process because of the release of chemically combined water. The simplest way for assessing the moisture change is monitoring the *mass loss*. Mass loss at high temperatures significantly depends on both chemical composition of ingredients and heating regimens.

The authors [8] used the characteristic length to assess concrete brittleness and found that the brittleness decreased with increasing heating temperature T_m and exposure time t_h. Using six energy-based and deformation-based toughness indices to examine similar phenomena, the authors [9,10] systematically studied the toughness of concrete under varied T_m, t_h and age based on a complete load–displacement curve in flexure. Recently, the authors measured fracture energy of high-performance concrete at high temperatures up to 450 °C [11]. In this paper, the effect of moisture loss on concrete brittleness due to heating is further studied from three-point bending tests on the preheated notched beams. The mass loss ω is also monitored during heating. Thus, relationships of the brittleness of the studied concrete with T_m, t_h, and ω can be finally established.

2. Brittleness index for concrete

A complete load–displacement curve in flexure (Fig. 1) comprises the initial stiffness K_0, the ultimate load P_u, the cracking displacement Δ_c, the failure displacement Δ_f, and other hardening and softening properties. Failure is defined as the point on the descending curve when load drops to zero. In this study, the ratio of the elastic energy A_e stored at peak load to the total energy A at failure is defined as a brittleness index B:

$$B = \frac{\text{Elastic energy}}{\text{Total energy}} = \frac{A_e}{A} = \frac{A_e}{A_a + A_d} \tag{1}$$

where $A_e = A_a - A_p$, A_a and A_p are the total energy and the plastic energy on the ascending branch, respectively; $A = A_a + A_d$ and A_d is the total energy on the descending branch; $\Delta_e = \Delta_c - \Delta_p$ is the elastic deformation and Δ_p is the plastic deformation on the ascending branch. For an elastic–plastic material, $B = 0$, and for an elastic–brittle material, $B = 1$.

Here, a two-function load–displacement relationship (P–Δ) is proposed as follows:

$$P = \begin{cases} P_u[1-(1-\Delta/\Delta_c)^{\alpha}] & \text{for } 0 \le \Delta \le \Delta_c \\ P_u \exp[-\beta(\Delta-\Delta_c)^{\gamma}] & \text{for } \Delta_c \le \Delta \le \Delta_f \end{cases} \tag{2}$$

where α is a hardening index ($\alpha \ge 1$); β is a softening coefficient ($\beta > 0$); γ is a softening index ($\gamma > 0$). Now we can integrate Eq. (2) to obtain A. If we assume that the

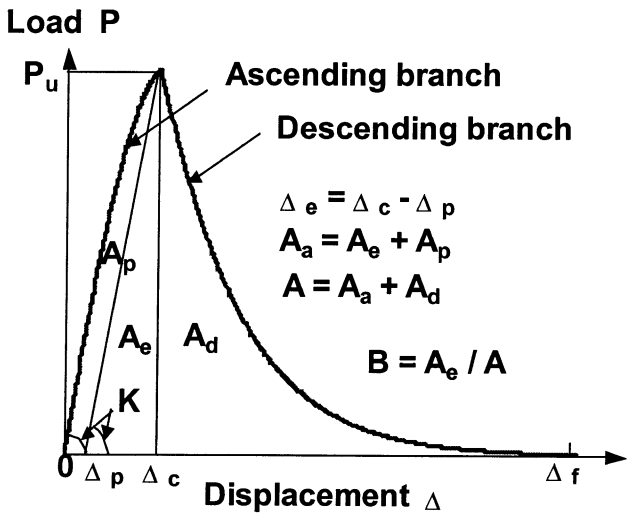

Fig. 1. A complete load–displacement curve for a notched beam.

unloading from the peak is linearly elastic with the same stiffness K_0, then we can get:

$$B = \frac{1}{\frac{2\alpha^2}{\alpha+1} + \frac{2\alpha}{\beta\frac{1}{\gamma}\gamma\Delta_c}\left\{\gamma\Gamma\left(1+\frac{1}{\gamma}\right) - \Gamma\left[\frac{1}{\gamma}, \beta(\Delta_f - \Delta_c)^{\gamma}\right]\right\}} \quad (3)$$

where $\Gamma(z) = \int_0^{\infty} x^{z-1}e^{-x}\mathrm{d}x$ is the Euler gamma function, and $\Gamma(a,z) = \int_z^{\infty} x^{a-1}e^{-x}\mathrm{d}x$ is the incomplete gamma function. In the previous study [9,10], P_u, Δ_c, Δ_f, α, β, and γ have been obtained as the functions of heating temperature (T_m) and exposure time (t_h):

$$P_u = 1.67(t_h+1)^{-7.26\times10^{-10}(T_m-T_0)^{3.36}} \quad \text{(kN)} \quad (4)$$

$$\Delta_c = 0.15(t_h+1)^{1.29\times10^{-3}(T_m-T_0)^{0.94}} \quad \text{(mm)} \quad (5)$$

$$\Delta_f = 1.18(t_h+1)^{2.97\times10^{-3}(T_m-T_0)^{0.80}} \quad \text{(mm)} \quad (6)$$

$$\alpha = 1.14(t_h+1)^{5.41\times10^{-6}(T_m-T_0)^{1.68}} \quad (7)$$

$$\beta = 4.53(t_h+1)^{-9.58\times10^{-5}(T_m-T_0)^{1.42}} \quad (8)$$

$$\gamma = 0.73(t_h+1)^{1.98\times10^{-3}(T_m-T_0)^{0.73}} \quad (9)$$

where T_0 is room temperature. Fig. 2 shows two typical families of complete load–displacement curves at varied heating temperatures and exposure times for the concrete in this study. In general, these curves are tall and spiky with sharp peaks at the start and become gradually shorter and more extended with increasing T_m and t_h. For any T_m or t_h, the brittleness index B can be uniquely determined using Eqs. (3)–(9).

3. Experimental program

In this study, three-point bending tests were conducted on preheated notched plain concrete beams of 500 × 100 × 100 mm with an effective span of 400 mm and a notch depth of 50 mm to obtain complete load–displacement curves. The beams were notched before being heated using a diamond saw. The concrete was made from rapid hardening Portland cement (BS Type III), siliceous quartz river sand, and 20 mm graded siliceous gravel at a ratio of 1:2.16:3.39. The water–cement ratio was 0.54 and the cement content was 335 kg/m^3. Specimens were first cured in the water tank at 20 ± 2 °C for 7 days and then moved out of the tank but still stored in the curing room until testing.

Concrete beams were heated in two ovens (100 ± 1 and 200 ± 1 °C) or one furnace (1000 ± 5 °C). The oven or furnace temperature T_m varied from 100 to 600 °C at an interval of 100 °C. As soon as the specified T_m levels were reached, the beams were placed in the oven or furnace and continuously heated. After the beams had been heated for a duration t_h, they were naturally cooled in the air for 12 h prior to the tests. Most beams were heated over a fixed time of 12 h at 14 days, and the remaining were heated over varied times up to 168 h from 14 days. For each heating regimen, at least three replicate specimens were tested for $T_m \le 200$ °C, but at least two for $T_m \ge 300$ °C. Three unheated beams were also tested for comparison. Thus, a total of 47 beams were tested in this study. The full test program is listed in Table 1.

The tests were conducted in a 2000-kN servo-controlled Losenhausen universal testing machine at a displacement rate of 1.25 μm/s until the beams were fully broken. The force P from the load cell and the displacement Δ of the machine were recorded. Since the net displacement of the beams was not measured, the load–displacement curves are approximations.

Two 100-mm cubes were cut from each broken beam: one for the compressive strength f_{cu} and the other for the splitting tensile strength f_t'. The mass of concrete beam

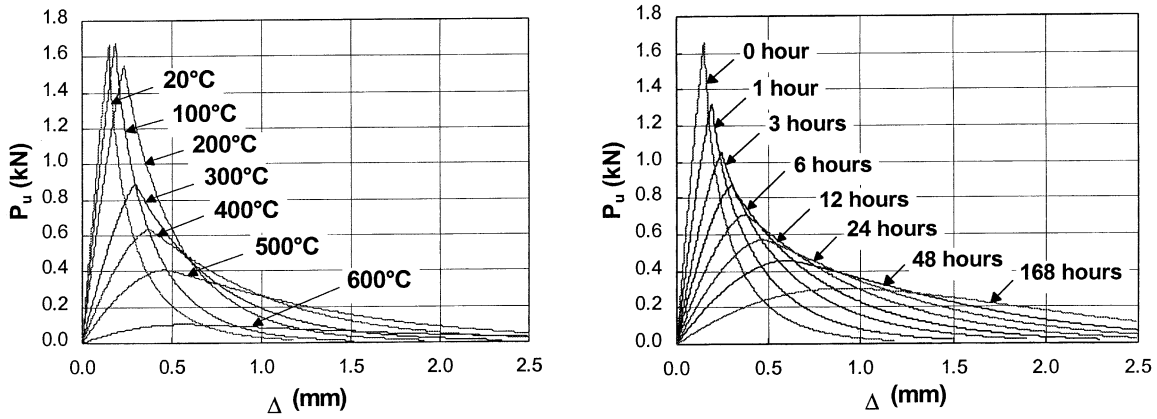

(a) For varied T_m at t_h = 12 hours (b) For varied t_h at T_m = 400°C

Fig. 2. Complete load–displacement curves for different values of T_m and t_h.

Table 1
Heating regimens and material properties

T_m (°C)	t_h (h)	Beam no.	ω (%)	f_{cu} (MPa)	f_t' (MPa)	f_r (MPa)	B
20	0	3	0.00	50.2 (4.1)	3.80 (6.4)	4.00 (2.0)	0.286
100	12	3	4.51 (4.6)	49.1 (4.9)	3.31 (6.2)	4.02 (6.4)	0.266
	24	3	5.55 (1.2)	50.6 (4.2)	3.33 (4.1)	4.04 (13.0)	0.261
	168	4	6.57 (0.9)	57.5 (4.2)	3.40 (5.9)	4.15 (10.9)	0.230
200	6	3	4.94 (0.9)	44.1 (5.1)	2.95 (8.5)	3.66 (6.0)	0.241
	8	3	5.72 (2.2)	49.6 (2.3)	2.96 (8.6)	3.68 (11.9)	0.221
	12	3	6.82 (5.7)	52.5 (3.5)	3.00 (0.7)	3.72 (0.9)	0.217
	168	4	7.76 (1.6)	59.5 (3.6)	3.20 (1.6)	3.87 (6.4)	0.211
300	12	2	7.39 (0.4)	48.4 (3.9)	2.49 (4.5)	2.13 (17.9)	0.147
	168	2	7.98 (1.0)	–	–	–	–
400	6	2	7.35 (1.8)	46.5 (7.0)	2.15 (2.6)	1.75 (23.5)	0.144
	12	2	7.76 (1.6)	44.0 (2.3)	1.89 (12.8)	1.52 (1.1)	0.122
	168	2	8.15 (2.0)	–	–	–	–
500	4	2	7.55 (2.9)	34.7 (4.9)	1.89 (13.7)	1.30 (12.3)	0.120
	12	2	8.46 (3.9)	32.6 (15.0)	1.36 (22.4)	0.98 (43.5)	0.102
	168	2	8.54 (4.2)	–	–	–	–
600	12	3	9.42 (0.4)	27.3 (32.1)	0.90 (33.7)	0.25 (23.3)	0.076
	168	2	9.47 (5.5)	–	–	–	–

The numbers in parentheses are the coefficients of variations (%).

specimens before heating and at different heating stages was monitored to determine ω using a factory balance of 15 kg ± 5 g. The modulus of rupture f_r is directly calculated from P_u. All test data are also listed in Table 1.

4. Mass loss during heating progress

4.1. ω vs. T_m

Fig. 3 shows the average ω values at different temperatures over 12 and 168 h. In general, ω increased with increasing T_m for both exposure times. This moisture loss process covers three typical stages. First, ω increased very rapidly with T_m until 200 °C mainly due to the evaporation of capillary water in concrete. This stage is a physical process because of the evaporation of macro capillary water. When T_m varied between 200 and 400 °C, ω was mainly caused by the evaporation of gel water and the evaporating rate became smaller because it would be more difficult for gel water to escape from gel pores with smaller sizes. This is a physical–chemical process due to the evaporation of meso gel water. At the third stage (over 400 °C), ω was mainly contributed to by the decomposition of hardened cement paste and aggregates so this is a chemical process due to the release of microchemically combined water. The test data can be expressed using a cubic polynomial relationship between ω and T_m as:

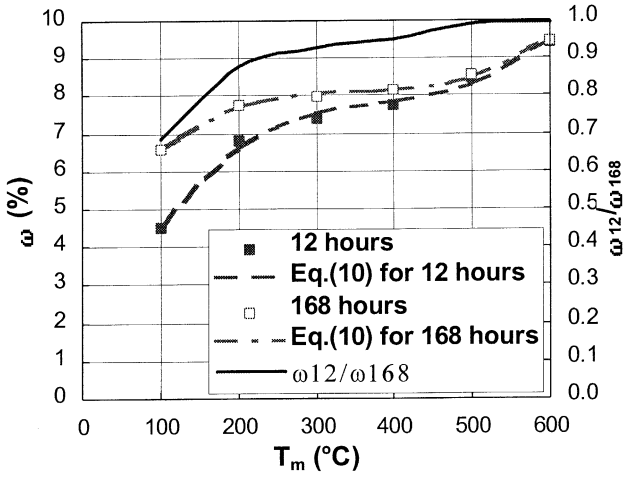

Fig. 3. Mass loss for different heating temperatures.

$$\omega = \begin{cases} 1.07\times10^{-7}T_m^{\,3} - 1.24\times10^{-4}T_m^{\,2} + 0.05T_m \\ \quad +0.67 \qquad \text{for } t_h = 12 \text{ h} \\ 7.74\times10^{-8}T_m^{\,3} - 8.24\times10^{-5}T_m^{\,2} + 0.03T_m \\ \quad +4.32 \qquad \text{for } t_h = 168 \text{ h} \end{cases} \tag{10}$$

The ratio of the mass loss for $t_h = 12$ h to that for $t_h = 168$ h is also plotted in Fig. 3. Here we assume the mass loss for $t_h = 168$ h as the *equilibrium mass loss* ω_e after which no further moisture will migrate from the concrete. This ratio increased with T_m, from 0.69 at 100 °C and 0.88 at 200 °C to 0.99 at both 500 and 600 °C. This means that it takes longer for moisture loss to stabilise at lower temperatures, but an exposure time of 12 h will be enough for higher temperatures (over 500 °C).

4.2. ω vs. t_h

The effect of the exposure time t_h on ω was investigated on the beams heated over varied exposure times up to 168 h for six heating temperatures from 100 to 600 °C. The mass loss was continuously monitored on the beams heated over 168 h up to 400 °C. Fig. 4 shows the continuous mass loss with increasing t_h up to 168 h. At 100–400 °C, the

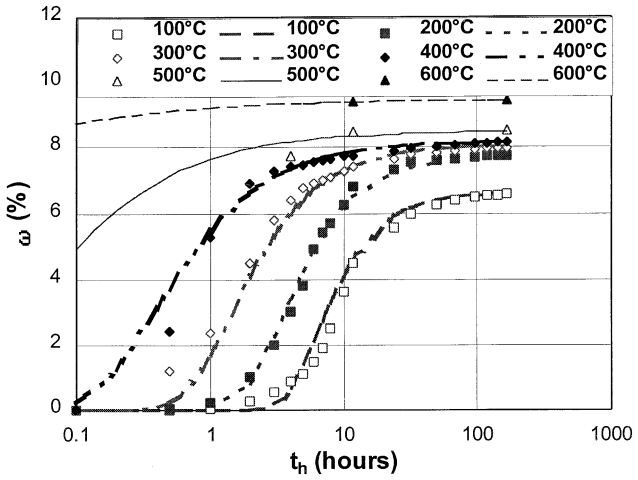

Fig. 4. Mass loss of concrete for different exposure times.

measurements were taken at $t_h = 0.5$ h, 1–8 h at an interval of 1 h, 10, 12, 24, 36, and 48–168 h (1 week) at an interval of 24 h. At 500 and 600 °C, the measurements were only taken at two exposure times. The symbols in Fig. 4 are the test results. In general, ω was a monotonically increasing function of t_h for each T_m, but the increase rate became smaller after 12 h. The moisture evaporation occurred in three stages. First, the evaporating rate was very small because the heat could only remove the moisture near the surface of the specimen. In the second stage, the moisture evaporated very quickly so ω increased rapidly. The temperature became gradually uniform in the specimens and drove out the moisture from the internal depth. Thereafter, the evaporating rate became smaller again and ω tended to be stable. The length of the first stage is greatly dependent on the heating temperature. It was about 1 h for 100 and 200 °C and less than half an hour for 300 and 400 °C, but only several minutes for higher heating temperatures. Normally, mechanical tests at high temperatures should be conducted when the moisture loss stops. The second stage can be used to design the heating program more effectively. To reach 95% of the equilibrium mass loss ω_e, we can find the corresponding t_h would be 48 h for 100 °C, 24 h for 200 °C, 10 h for 400 °C, and even shorter exposure times for higher temperatures. Of course, the actual heating duration for such moisture state also greatly depends on the concrete composition and the specimen geometries.

The mass loss during heating for a given temperature can be expressed using an exponential relationship between ω and t_h as:

$$\omega = a_{wt}\exp(-b_{wt}/t_h^{c_{wt}}) \quad (11)$$

where a_{wt}, b_{wt}, and c_{wt} are constants. When $t_h \to 0$, $\omega \to 0$, which defines the unheated state. When $t_h \to \infty$, $\omega \to a_{wt}$, which defines the equilibrium state. a_{wt} is equal to *the equilibrium mass loss* ω_e and can be determined using Eq. (10). After ω_e is known, b_{wt} and c_{wt} can be determined using linear regression. Table 2 lists the calculated constants and the corresponding correlation coefficients r for each heating temperature. As shown in Eq. (10) and Fig. 3, a_{wt} is a monotonically increasing function of T_m, but b_{wt} and c_{wt} decrease with T_m (see Table 2). Here b_{wt} and c_{wt} are estimated as (Eqs. (12) and (13)):

Table 2
Best-fit values of coefficients for determining ω at different temperatures

T_m (°C)	a_{wt} (%)	b_{wt}	c_{wt}	r
100	6.57	25.320	1.662	0.992
200	7.76	5.813	1.463	0.995
300	7.98	1.327	1.193	0.984
400	8.15	0.456	0.953	0.967
500	8.54	–	–	–
600	9.47	–	–	–

$$b_{wt} = 90.403\exp(-0.0135T_m) \quad (12)$$

$$c_{wt} = 1.917 - 2.396\times10^{-3}T_m \quad (13)$$

Eq. (11) is also plotted in Fig. 4 and predicts the test results quite well.

5. Concrete strengths for different heating temperatures

Fig. 5 shows the ratios of three strengths for different heating temperatures over a 12-h exposure time to the corresponding strengths at room temperature. f_{cu} changed very little with T_m below 200 °C because lower heating temperatures helped the further hydration, thereby increasing the overall strength. This strengthening effect could well balance the strength loss caused by thermally induced microcracks. The maximum of f_{cu} occurred at 200 °C with a net increase of 5%. Thereafter, f_{cu} gradually decreased with T_m because more damaging microcracks were induced and

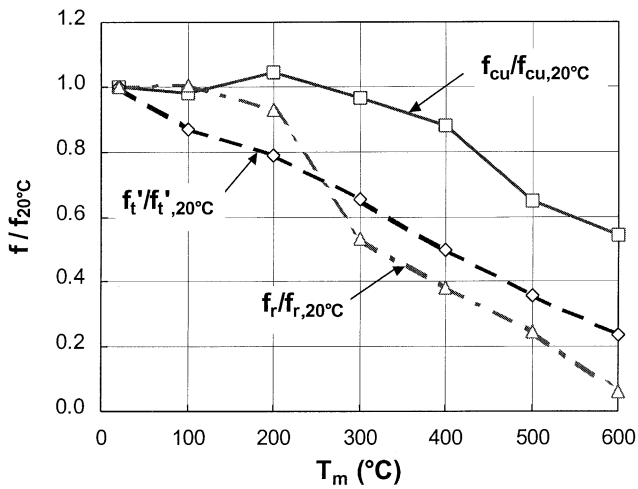

Fig. 5. Concrete strengths for different heating temperatures and 12 h exposure.

had a net drop of 46% at 600 °C. f_t' decreased with increasing T_m continuously and dropped by 76% at 600 °C. f_r did not change when T_m increased to 100 °C, and slightly decreased at 200 °C. Thereafter, f_r sharply decreased with T_m, down by 94% at 600 °C. The drop in f_t' was always larger than that in f_r for $T_m \leq 200$ °C, but became smaller for $T_m \geq 300$ °C because the higher temperatures induced not only global microcracks but also serious local cracks near the notch tip. Thus, the flexural resistance would be significantly reduced.

6. Brittleness for different heating regimens

Based on Eqs. (5)–(9) for the parameters Δ_c, Δ_f, α, β, and γ, which depend on T_m and t_h, we can determine the brittleness index B using Eq. (3). In Fig. 6, the experimental data show that for $t_h = 12$ h at 14 days, B decreases monotonically with increasing T_m, and the decrease rate gradually increased after 200 °C but became slightly smaller after 400 °C. When T_m varied from 20 to 600 °C, B decreased from 0.286 to 0.076, down by 73% at 600 °C. Higher temperatures always decrease the elastic deformation and elastic energy of concrete but greatly increase the irrecoverable plastic deformation and absorbed energy (on both ascending and descending branches). Therefore, the change in the proportion of the elastic energy to the total energy can represent the change in the brittleness of concrete subject to heating temperatures. Meanwhile, microcracks due to the heating–cooling process can make the actual cracking surface much larger than the nominal one and consumes more irrecoverable energy. The interlock effect due to these thermal cracks becomes greater and consumes more energy as well.

Fig. 7 shows the variation of B with t_h for 100–600 °C at 14 days based on Eq. (3). The symbols are the individual values of B derived from the test data. B monotonically decreases with t_h. Longer exposure time for each heating temperature decreases the elastic deformation and elastic energy of concrete but greatly increases the irrecoverable plastic deformation and absorbed energy. However, the decrease rate of concrete brittleness with t_h is not uniform over the whole exposure time but decreases with increasing t_h. At the start of heating, the decrease rate is very large over 12 h, but becomes smaller thereafter. In other words, the most loss in brittleness happens within the first 12 h of exposure. For example at 200 °C, B decreases from 0.286 to 0.217 over 12 h and to 0.211 over 168 h, down by 24.1% and 26.2%, respectively. Meanwhile, the decrease rate at any exposure time is always greater for higher temperatures.

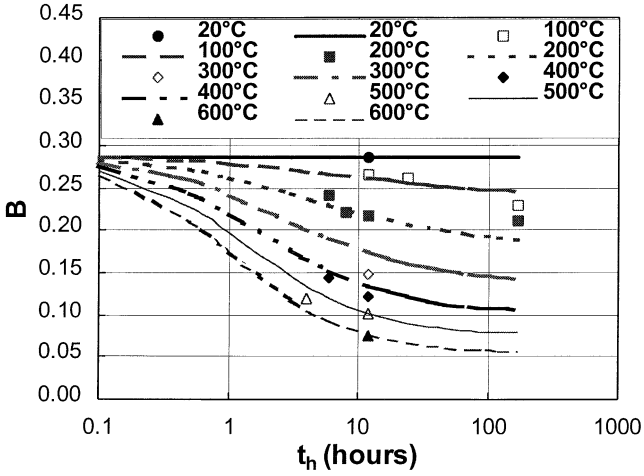

Fig. 7. Concrete brittleness for different exposure times at varied temperatures.

7. Brittleness and mass loss

7.1. B vs. ω for different heating temperatures

Fig. 8 shows the variation of B with mass loss ω for different heating temperatures with the test data shown as

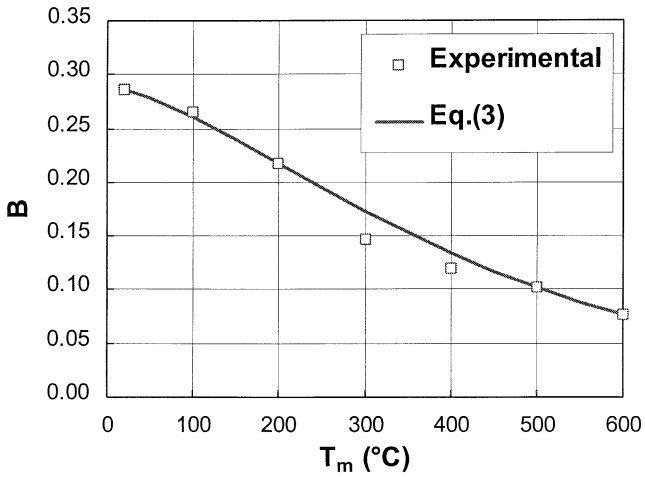

Fig. 6. Concrete brittleness for different heating temperatures and 12 h exposure.

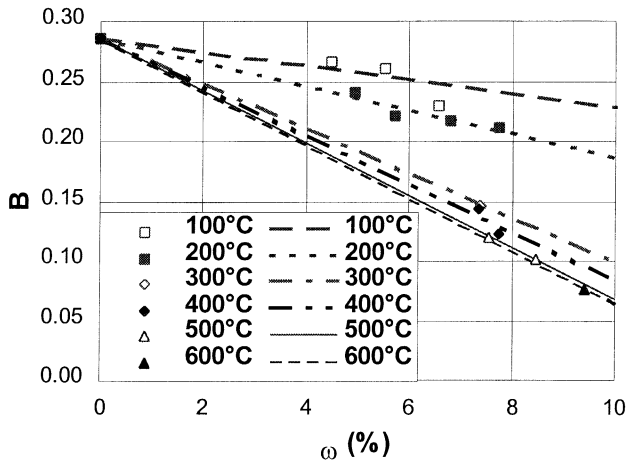

Fig. 8. Relationship between brittleness and mass loss for different heating temperatures.

symbols. For each T_m, B decreased monotonically with increasing ω due to increasing exposure times. This means that the evaporation of moisture reduced the brittleness of concrete. Here, one constant value of ω corresponds to different B values for different temperatures. The higher the heating temperature, the smaller the value of B. Actually, higher heating temperature not only accelerates the loss of moisture in the concrete, but also causes more microstructural changes and creates more microcracks on the interface between cement paste and aggregates and in the cement paste and aggregates. These cracks cause the brittleness to decrease. Higher heating temperature also removes hydration water and reduces the concrete strength, but the brittleness is more closely related to the change in deformation rather than to the change in load. From the definition of brittleness, the proportion of the elastic energy to the total energy, i.e., the brittleness, is more related to the proportion of the elastic deformation to the failure deformation if the load term is approximately eliminated.

For each T_m, the decrease of B with increasing ω was approximately linear, so we can assume a linear relationship between B and ω for each T_m as:

$$B = a_{b1} + b_{b1}\omega \tag{14}$$

where a_{b1} and b_{b1} are constants. When $\omega = 0$, $B = a_{b1}$, so a_{b1} defines the brittleness of concrete at room temperature which is 0.286 in this study. b_{b1} is the slope for B–ω curves, so $b_{b1} = dB/d\omega$. We can obtain the values of $dB/d\omega$ for different temperatures based on the test data, which are listed in Table 3. It can be seen that $dB/d\omega$ decreased very quickly with increasing T_m until 300 °C and thereafter the decrease rate became smaller. This trend can be expressed using an exponential $dB/d\omega$–T_m relationship as (Eq. (15)):

$$dB/d\omega = a_{b2}\exp[-b_{b2}/(T_m - 100)^{c_{b2}}] + d_{b2} \tag{15}$$

where a_{b2}, b_{b2}, c_{b2}, d_{b2} are constants, $b_{b2} > 0$ and $T_m \geq 100$ °C. When $T_m = 100$ °C, $dB/d\omega = d_{b2} = (dB/d\omega)_{100\ ^\circ C}$. When $T_m \to \infty$, $dB/d\omega = a_{b2} + d_{b2} = (dB/d\omega)_{\infty}$, so this sum defines the slope when T_m is very high. Here we assume that $(dB/d\omega)_{\infty} = \lambda(dB/d\omega)_{600\ ^\circ C}$ where λ is a constant and $\lambda \geq 1$. Thus, we have $a_{b2} = \lambda(dB/d\omega)_{600\ ^\circ C} - d_{b2}$. Both $(dB/d\omega)_{100\ ^\circ C}$ and $(dB/d\omega)_{600\ ^\circ C}$ can be chosen from Table 3. Using linear regression, we can find b_{b2} and c_{b2} if we choose a λ value to obtain a maximum correlation coefficient. Here we obtain $\lambda = 1.045$, $a_{b2} = 0.018$, $b_{b2} = 10780$, $c_{b2} = 1.95$, and $d_{b2} = 0.0058$ with $r = 0.994$.

Table 3
$dB/d\omega$ for different heating temperatures

T_m (°C)	100	200	300	400	500	600
$dB/d\omega$	−0.00582	−0.01006	−0.01881	−0.02023	−0.02187	−0.02229

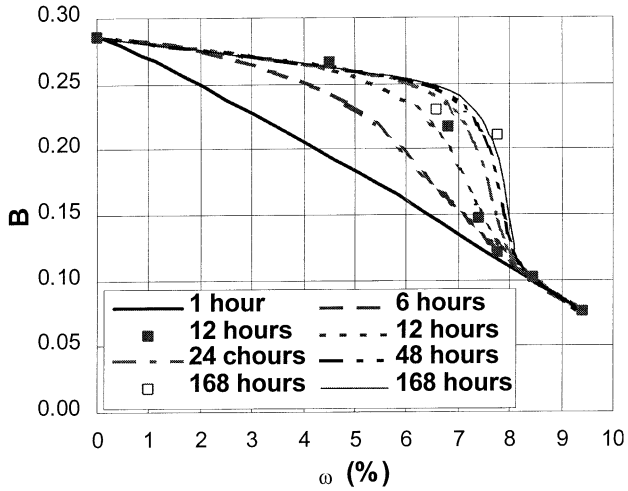

Fig. 9. Relationship between brittleness and mass loss for different exposure times.

As shown in Figs. 3 and 4, the exposure time affects the mass loss in the intermediate stages and finally stabilises the moisture loss if it is long enough. Heating temperature, however, determines the magnitude of mass loss for the equilibrium state. As shown in Figs. 6 and 7, the exposure time only reduces concrete brittleness to a certain degree, but higher heating temperatures cause more reduction in concrete brittleness if the exposure time is long enough. Thus, the heating temperature is more influential on the moisture state and brittleness of concrete and on their relationship than the exposure time.

7.2. B vs. ω for different exposure times

Fig. 9 shows B with ω for different exposure times based on Eqs. (11) and (14). The exposure time t_h is chosen as 1, 6, 12, 24, 48, and 168 h. For each t_h, B decreases monotonically with increasing ω due to increasing heating temperatures. When $t_h = 1$ h, B decreases almost linearly with ω. With increasing t_h, the B–ω curve becomes more nonlinear and moves up towards the right quickly until $t_h = 12$ h. Thereafter, such additional movement becomes small, and an equilibrium state is reached for $t_h = 168$ h. The change in the curve shape in the first 12 h is more significant than that between 12 and 168 h. This is essentially caused by the difference in heating temperatures. Lower temperatures only cause small mass loss in the first few hours, but this significant change is mainly due to higher temperatures. After 24 h, the curve is almost unchanged. This proves again that an exposure time of 12 h (except at lower heating temperatures below 200 °C) is sufficient for obtaining an equilibrium state.

If we look at the shape of the B–ω curves after 12 h of expose more closely, we can see there exist three stages for ω. In the first stage, ω varies from 0% to 4.5% and B slightly decreases with ω. The relationship between B and ω is slightly dependent on t_h. In this stage, only capillary water

evaporates under relatively low heating temperatures, which does not cause significant structural damage. The $B-\omega$ relationship is unchanged for different exposure times. In the second stage, ω varies from 4.5% up to 8.5%, and B decreases with ω at an increasing rate. This stage is greatly dependent on t_h. With increasing t_h, the curve moves up towards the right. For a constant B, longer exposure time causes larger mass loss that should instead decrease concrete brittleness. It is even interesting to see for a constant ω, longer exposure time that should decrease brittleness causes instead larger brittleness. This is again because the heating temperature plays a dominant role. In this stage, mainly gel water evaporates, but its dissipation rate depends on heating regimens. Heating over a shorter time at higher temperatures normally induces more microstructural damage that causes less brittleness than heating over longer exposure time at lower temperatures. In the third stage with $\omega > 8.5\%$, the relationship between B and ω appears unchanged with t_h, and B monotonically decreases with increasing ω. This stage is only applicable for higher heating temperatures because lower temperatures never cause that big mass loss. Most gel water has evaporated now, so the further loss of moisture is merely contributed to by the release of chemically combined water in decomposition.

8. Discussion

This study suggests that the evaporation of moisture from concrete exposed to high temperatures decreases the brittleness. This may not be immediately obvious, but the reason for this can be traced to changes in microstructure. At micro level, the mechanical properties of a material are governed by the combining states of its molecules and atoms. The interconnecting force of atoms comes from the atomic static electricity and includes primary bonds (ionic bond, covalent bond, and metallic bond) and secondary or molecular bonds (van der Waals' bond and hydrogen bond). Primary bonds have strong bonding ability and the bond energy varies from 5 to 12 kJ/mol. Ionic bonds are nondirectional and nonsaturable, while covalent bonds are directional and saturable and can only combine with one another along certain directions. Secondary bonds have weak bonding ability and the bond energy only varies from 0.2 to 2.4 kJ/mol. Most concrete-like materials actually consist of different types of bonds. The brittleness of a material essentially lies in the directionality and saturability of covalent bond and hydrogen bond. Hence, the essential step to improve the brittleness is to reduce the proportions of covalent and hydrogen bonds and to increase the proportions of ionic, molecular, and metallic bonds.

Water is neither purely ionic nor purely covalent and is commonly described as a polar covalent compound. In each water molecule, two hydrogen atoms combine with an oxygen atom at an angle of 105°. This gives water an asymmetric distribution of charge, i.e., molecules have ends with partial negative and positive charges known as polar molecules. The positively charged regions in one water molecule will attract the negatively charged regions in other water molecules by hydrogen bond in which a hydrogen atom is shared by two other atoms. Even though hydrogen bonds are much weaker than covalent bonds, a large number of hydrogen bonds will make a strong contributory effect when they act in unison.

Concrete is a heterogeneous multiphase material with relatively inert aggregates cemented together by hydrated Portland cement paste. Mature cement paste is normally composed of 70–80% layered C-S-H gel, 20% $Ca(OH)_2$, and other chemical compounds [13]. A C-S-H gel structure is made of three types of groups that contribute to bonds across surfaces or in the interlayer of partly crystallised, malformed tobermorite-like material: calcium ions, siloxanes, and water molecules. The boding of the water within the layers also called gel water with other groups via hydrogen bond determines the properties of concrete such as strength, stiffness, creep, swelling, but also affects the toughness and brittleness of concrete due to the directionality and saturability of hydrogen bond. Earlier studies suggest that the absorbed water along the C-S-H gel sheets seems hardly to affect these properties. In this study, the test results of the brittleness with the mass loss of concrete exposed to high temperatures have confirmed this. The evaporation of capillary water from concrete at varied heating temperatures did not cause significant decrease in the brittleness, but the evaporation of gel water significantly decreased the brittleness. Further slight decrease in the brittleness was mainly caused by decomposition. This strongly implies that the existence of gel water in concrete is the main cause of its higher brittleness. The simplest way to improve the concrete brittleness is to reduce the content of gel water but this unavoidably decreases the strength. Therefore, other ways have to be adopted for substituting rather than decreasing the gel water so as to improve the strength and to decrease the brittleness. So far, polymer impregnated mortar and concrete has been successfully developed for such propose. This greatly reduces the porosity and also changes the bonding because the gel water is replaced by long-chain polymers. The proportions of molecule bonds and freely turning covalent bonds greatly increase so as to reduce the directionality. Thus, the concrete strength [14], stiffness [14], and toughness [15] could increase and the brittleness [16] could decrease.

It is known that the evaporation of gel water significantly decreases the strength of concrete exposed to high temperatures. Some other substitutes rather than polymers can possibly be found to replace the gel water to further strengthen the concrete at high temperature because the polymers cannot sustain high temperatures.

Earlier on references were made to two types of brittleness for concrete: material brittleness and structural brittleness. The change of geometric dimensions in concrete

structures is the cause for the latter. Here only the material brittleness is studied, but the definition of brittleness in Eq. (1) is universal and can be used to assess the geometric brittleness. The simplest example is that a longer specimen under direct tension or compression shows more brittle feature at failure than the shorter one made of the same material because it contains a larger proportion of the elastic energy to the total energy.

9. Conclusions

To sum up, the effect of moisture loss on concrete brittleness at high temperatures incorporating different exposure times has been investigated on preheated concrete beams. The mechanism of concrete brittleness and the possible application of this study have also been discussed. This can help further understand cracking and failure of concrete, develop new extremely strong and ductile materials, and achieve better and more logical and holistic design. The following conclusions can be drawn.

• Mass loss is a parameter that can help distinguish three different regimens. When the heating temperature is below 200 °C, the mass loss is caused entirely by the quick evaporation of capillary water so the concrete sustains a physical process. For temperatures between 200 and 400 °C, the mass loss is mainly caused by the gradual evaporation of gel water and the concrete sustains a mixed physical–chemical process. For temperatures over 400 °C, the mass loss is mainly contributed to by the loss of chemically bound water (dehydration and decomposition) so the concrete sustains a chemical process. Longer exposure time always causes larger mass loss. However, an exposure time of 12 h can allow an equilibrium state to be reached for higher heating temperatures.

• The energy-based brittleness index covers the whole failure process (ascending and descending branches) so its change can be used to assess the brittleness of concrete exposed to high temperatures. Higher heating temperature always leads to lower brittleness. Longer exposure time at a given temperature also leads to lower brittleness, but this effect is more significant at early exposure stage under 12 h and becomes less influential thereafter.

• The loss of moisture from concrete due to heating always leads to a decrease in the brittleness. There is a linear relationship between the brittleness and the mass loss for each heating temperature. If the exposure time is long enough (over 12 h), there also exist three stages as described above. In the first and third stages, the heating regimens have a small influence on the relationship between the brittleness and the mass loss, but become more influential in the second stage. In other words, the existence of gel water significantly influences the brittleness of concrete.

Acknowledgments

This work was partly carried out under the British Energy contract PP/120543/DGD/HN.

References

[1] B. Zhang, Z. Zhu, Study on fatigue damage in concrete pavements, J Chin. Civ. Eng. 19 (4) (1986) 54–60 (in Chinese).
[2] Y. Yu, Y. Zhang, Stability analysis of vertical cracks on upstream face of diamond head buttressed dam at Zhexi Hydropower Station, in: F.H. Wittmann (Ed.), Fracture Toughness and Fracture Energy of Concrete, Elsevier, Amsterdam, The Netherlands, 1986, pp. 597–606.
[3] H.H. Bache, Model for strength of brittle materials built up of particles jointed at points of contact, J Am. Ceram. Soc. 53 (12) (1979) 654–658.
[4] Z.P. Bazant, M.F. Kaplan, Concrete at High Temperatures: Material Properties and Mathematical Models, Longman, England, 1996.
[5] RILEM Committee 44-PHT, in: U. Schneider (Ed.), Behaviour of Concrete at High Temperatures, Department of Civil Engineering, Kassel University, Kassel, Germany, 1985.
[6] U. Schneider, Concrete at high temperatures — a general review, Fire Saf. J. 13 (1988) 55–68.
[7] L.T. Phan, N.J. Carino, Review of mechanical properties of HSC at elevated temperature, J. Mater. Civ. Eng., ASCE 10 (1) (1998) 58–64.
[8] B. Zhang, N. Bicanic, C.J. Pearce, G. Balabanic, Residual fracture properties of normal and high strength concrete subjected to elevated temperatures, Mag. Concr. Res. 52 (2) (2000) 123–136.
[9] B. Zhang, N. Bicanic, C.J. Pearce, G. Balabanic, Assessment of concrete brittleness subjected to elevated temperatures: Part 1. General introduction, ACI Mater. J. 97 (5) (2000) 550–555.
[10] B. Zhang, N. Bicanic, C.J. Pearce, G. Balabanic, Assessment of toughness of concrete subjected to elevated temperatures: Part 2. Experimental investigations, ACI Mater. J. 97 (5) (2000) 556–566.
[11] B. Zhang, N. Bicanic, Fracture energy of high performance concrete at temperatures up to 450 °C, Proceedings of the 4th International Conference on Fracture Mechanics of Concrete and Concrete Structures, Cachan, France, 28 May–1 June 2001, A.A. Balkema Publishers, Lisse, The Netherlands, 2001, pp. 461–468.
[12] B. Zhang, N. Bicanic, C.J. Pearce, G. Balabanic, Discussion on the paper "Residual fracture properties of normal and high strength concrete subjected to elevated temperatures", Mag. Concr. Res. 53 (3) (2001) 221–224.
[13] V.S. Ramachandran, R.F. Feldman, J.J. Beaudoin, Concrete Science — Treatise on Current Research, Hey & Son, England, 1981.
[14] J. Manson, W. Chen, J. Vanderhoff, H. Mehta, P. Cady, D. Kline, P. Blankenhorn, Use of Polymers in Highway Concrete, NCMRP Report 190, Transport Research Board NRC, 1978.
[15] J. Clifton, J. Fearn, E. Anderson, Polymer Impregnated Hardened Cement Pastes and Mortars, US Department of Commerce, NBS, Building Science Series 83, 1976.
[16] Y.-Y. Huang, K. Wu, M. Tan, Z. Shen, The mechanisms of modification in mechanical behaviour of PCC, PIC and PI (PCC), Proceedings of the 4th International Conference on Polymer Concrete, Ducke Offsetdruck GmbH, Darmstadt, Germany, 1984, pp. 429–433.